FIELD OBSERVATIONS USING AN AOTF POLARIMETRIC IMAGING SPECTROMETER

Li-Jen Cheng, Mike Hamilton, Colin Mahoney, and George Reyes
Jet Propulsion Laboratory, California Institute of Technology
Pasadena, CA 91109

1. INTRODUCTION

This paper reports preliminary results of recent field observations using a prototype acousto-optic tunable filter (AOTF) polarimetric imaging spectrometer. The data illustrate application potentials for geoscience.

The operation principle of this instrument is different from that of current airborne multispectral imaging instruments, such as AVIRIS. The AOTF instrument takes two orthogonally polarized images at a desired wavelength at one time, whereas AVIRIS takes a spectrum over a predetermined wavelength range at one pixel at a time and the image is constructed later. AVIRIS does not have any polarization measuring capability. The AOTF instrument could be a complement tool to AVIRIS.

Polarization measurement is a desired capability for many applications in remote sensing. It is well known that natural light is often polarized due to various scattering phenomena in the atmosphere. Also, scattered light from canopies is reported to have a polarized component (Vanderbilt et al., 1988). To characterize objects of interest correctly requires a remote sensing imaging spectrometer capable of measuring object signal and background radiation in both intensity and polarization so that the characteristics of the object can be determined. The AOTF instrument has the capability to do so.

The AOTF instrument has other unique properties. For example, it can provide spectral images immediately after the observation. The instrument can also allow observations to be tailored in real time to perform the desired experiments and to collect only required data. Consequently, the performance in each mission can be increased with minimal resources.

The prototype instrument was completed in the beginning of this year. A number of outdoor field experiments were performed with the objective to evaluate the capability of this new technology for remote sensing applications and to determine issues for further improvements.

2. ACOUSTO-OPTIC TUNABLE FILTER

The AOTF consists of a birefringence crystal to which one or several piezoelectric transducers are bonded. When a RF signal is applied, the transducer generates acoustic waves launching into the crystal. The propagating acoustic waves produce a periodic modulation of the index of refraction. This provides a moving phase grating that diffracts portions of an incident light beam. For a fixed acoustic frequency, only a narrow band of optical frequencies can approximately satisfy the phase-matching condition and be collectively diffracted. As the RF changes, the center of optical bandpass changes accordingly. This creates a tunable bandpass filter.

In a birefringence crystal, there are two types of light waves, ordinary and extraordinary, with polarization orthogonal to each other. In an AOTF, the grating

diffracts an ordinary wave into an extraordinary wave and vice versa. If the incident beam is unpolarized, there will be two orthogonally polarized diffracted beams exiting at the opposite sides of the undiffracted beam, as illustrated in Figure 1. This provides opportunities to measure polarization of incident light.

3. PROTOTYPE SYSTEM

The system contains an optical subsystem, two integrating CCD cameras, a RF generator and a power amplifier, a 386 IBM-PC compatible computer for control and data acquisition and monitors. The unique part of the system is the optical configuration as illustrated in FIGURE 2. It contains a 3 inch aperture, zoom telelens set with variable focal length of 80-120 mm as the objective lens; an aperture located at the objective lens image plane for allowing only photons from the desired scene to pass through; a collimating lens (f=40mm) to create an intermediate pupil plane whose cross section is comparable with that of an AOTF; an AOTF located at the pupil plane, a field lens to create adequate beam diversion for imaging at the cameras; and two cameras for recording two polarized images separately. The operation wavelength of this instrument is 0.48-0.77 microns. A more detailed description of the system was published in a recent paper (Cheng et al., 1993).

4. EXPERIMENTAL RESULTS

Several outdoor observations were performed at JPL and Ft. Huachuca, AZ during sunny days. Figure 3 gives a picture of the scene in a raw country site of Ft. Huachuca. Many interesting features in the scene were observed. Because of the page limitation, some of them are reported here as an illustration. A reflection reference plate of $BaSO_4$, observable as a small bright rectangular object in the upper left part of the picture, was put in the scene for intensity normalization among images taken at different wavelengths. The distance between the plate and the instrument was about 3.5 km.

After the observations, image data were transferred to a 33 MHz 486 computer for data normalization, image cube formation, and data analysis using the interactive data language (IDL) in the MS window environment.

The scene can be approximately divided into three areas: 1) a vegetation rich area covering the lower part of the picture, 2) a wide open area with reddish soil, dry grass, a dirt road, and a few bushes, located above the first area, and 3) a ridge, across the top of the picture, with a mixture of trees and dry grass.

In the left part of Area 1, there is a group of trees, possibly local oak trees. From their appearance, there are two types of trees in the group. One has a bright green color and is named Tree 1. The other has a grayish green color and is named Tree 2. Figures 4 and 5 give typical observed spectra of Tree 1 and Tree 2, respectively. In comparison, Tree 1 has high reflection in the near infrared wavelength region and high absorption around 0.68 micron, due to chlorophyll, whereas Tree 2 has low reflection in the infrared and low absorption around 0.68 micron. If Tree 1 and Tree 2 belong to same species, one could conclude that Tree 2 is not in a healthy state.

Figure 6 shows a pair of observed spectra at a distant tree on the ridge at the far upper left corner of Figure 3. In comparison with the spectra in Figure 4, one easily noted feature is that the measured intensities of the spectra become significantly higher as wavelength decreases. This observation and high background intensities in all measured spectra are consistent with the thought that a considerable amount of scattered

light due to dust and aerosols in air was added to the measured sign. The existence of haze in the air was also noticed in a color picture of the scene taken by an ordinary camera.

The map of vegetation is an important subject for earth sciences. The spectral derivative method is known to be an effective way of evaluating canopies (Wessman, 1990). One effective way to obtain a vegetation map is to make an image of spectral derivatives from the observed image cubes at a chlorophyll red edge wavelength. Figure 7 shows a spectral derivative image at 0.7 micron generated from the data. The image is a map of chlorophyll or the vegetation index. The bright parts correspond to canopies with sharp red edge absorption. These canopies also have higher measured reflection in the near-infrared wavelength region. Most parts of Area 2 are dark, as expected because the surface contains mostly bare soil and dry grass. There are several man-made objects, such as two cars and an antenna disk, which become invisible.

The spectral data in Figures 4-6 show considerable differences in signal intensity between two polarizations. The intensity minimum of the chlorophyll absorption at the vertical polarization shifts slightly toward longer wavelength with respect to that at horizontal polarization. The observation of this shift is consistent with the existence of high background light due to scattered light from dust and aerosols in the air. The polarization phenomena in the atmosphere near the surface are very complicated. The data observed so far do suggest that vegetation could have characteristic polarization spectra. This is a subject requiring more studies.

5. CONCLUSION

The preliminary results stated in this paper have illustrated the capability of the AOTF instrument in remote sensing by taking both intensity and polarization parameters. This new capability will create new opportunities for advancing geoscience as well as many other fields.

6. ACKNOWLEDGMENTS

The research described in this paper was performed by the Center for Space Microelectronics Technology, Jet Propulsion Laboratory, California Institute of Technology, under a contract with the National Aeronautics and Space Administration, and was jointly sponsored by the Army Space Technology and Research Office and the Planetary Instrument Definition and Development Program, National Aeronautics and Space Administration.

7. REFERENCES

Cheng, L.J., T.H. Chao, M. Dowdy, C. Labaw, C. Mahoney, G. Reyes, K. Bergman, "Multispectral Imaging Systems Using Acousto-Optic Filter", SPIE Proceedings, Vol. 1874, p. 224-231 (1993).

Vanderbilt, V.C. and K.J. De Venecia, 'Specular, Diffuse, and Polarized Imagery of an Oat Canopy', IEEE Trans. Geoscience and Remote Sensing, Vol. 26, p. 451-462 (1988).

Wessman, C.A., 'Evaluation of Canopy Biochemistry' in 'Remote Sensing of Biosphere Functioning', edited by R.J. Hobbs and H.A. Moony (Springer-Verlag, New York, 1990), p. 135-156.

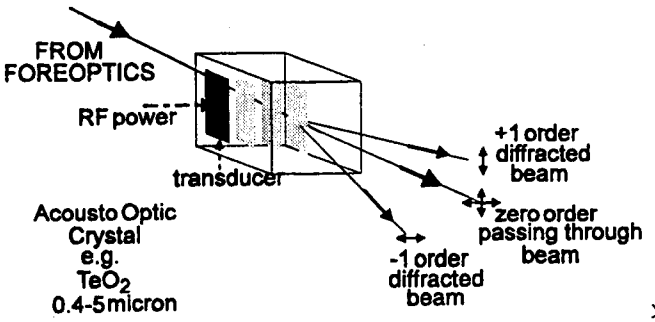

Figure 1. Schematic of a non-collinear AOTF.

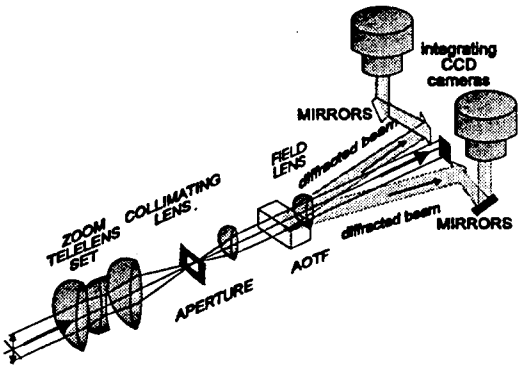

Figure 2. Schematic diagram of the ground system optical configuration.

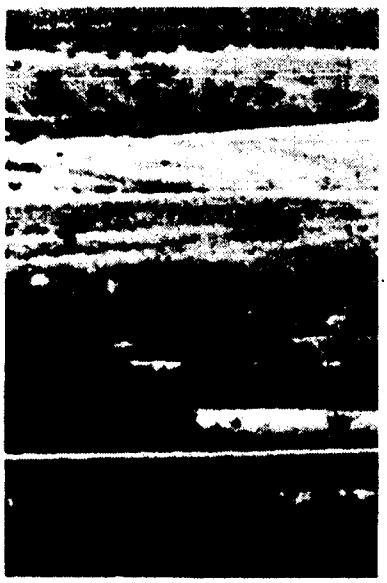

Figure 3. Picture of the scene studied.

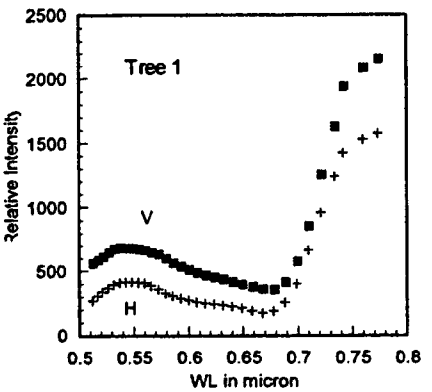

Figure 4. Spectra of Tree 1 with vertical and horizontal polarization

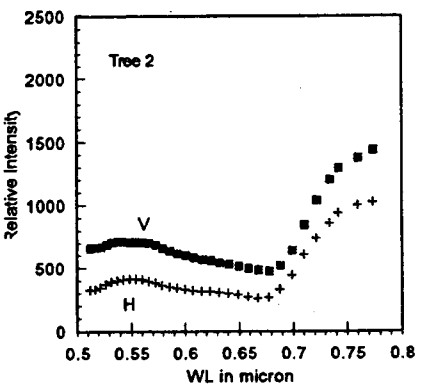

Figure 5. Spectra of Tree 2 with vertical and horizontal polarization

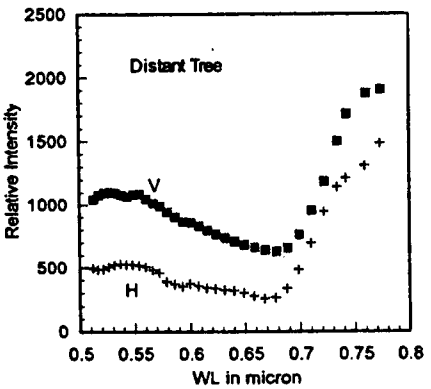

Figure 6. Spectra of distant tree with vertical and horizontal polarization

Figure 7. Derivative spectral image at 0.7 micron